VNU Journal of Science: Mathematics - Physics

Journal homepage: https://js.vnu.edu.vn/MaP

Original Article

A New Design of Ultra-flat Dispersion Photonic Crystal Fiber using Benzene Infiltration

Hoang Trong Duc[1], Nguyen Anh Tu[2], Nguyen Thi Thuy[1,*]

[1]*University of Education, Hue University, 34 Le Loi, Hue City, Vietnam*

[2]*Duc Pho High School, Duc Pho, Quang Ngai, Vietnam*

Received 12 July 2022
Revised 23 August 2022; Accepted 24 August 2022

Abstract: This paper presents new results on dispersion in photonic crystal fibers (PCF) based on a circular lattice, with benzene infiltration into the hollow-core. We achieved near-zero, ultra-flat dispersion through the appropriate adjustment of air hole diameters and pitch of cladding. The result gives a dispersion of ±0.484 ps/nm^{-1}.km over a wavelength range of 450 nm. Besides, we also obtained very high nonlinear coefficients, up to several thousand W^{-1}.km^{-1}, and a very low attenuation, about 10^{-21} dB/m for optimal structures suitable for supercontinuum generation application.

Keywords: PCF, benzene infiltration, ultra-flat dispersion, high nonlinear coefficients, low attenuation, supercontinuum generation.

1. Introduction

Photonic crystal fiber (PCF) [1] has been an attractive nonlinear medium for laser pulse propagation in supercontinuum (SC) generation studies, because it fulfills the requirements of low power and increasing the nonlinear effects [2]. The task of controlling the chromatic dispersion and increasing the nonlinearity of PCF has been the goal of the research groups. Recently, some publications mentioned two ways to efficiently control the chromatic dispersion and nonlinear properties of PCF suitable for SC applications. First, the lattice structure of PCF is suitably modified by varying the shape, size, and position of air-holes in the microstructured cladding, as shown in the selection of lattice types such as square [3], circle [4], hexagon [5], suspended core [6], etc. and the change of lattice parameters such as

* Corresponding author.
E-mail address: ntthuy@hueuni.edu.vn

https//doi.org/10.25073/2588-1124/vnumap.4762

hole diameter (d), core diameter (D_c), pitch (Λ) [7]. Second, the highly nonlinear liquids are infiltrated into the hollow core of PCFs [4, 8-12].

The interaction of the laser pulse with a highly nonlinear medium such as PCF is strongly influenced by dispersion properties, as a result, various nonlinear effects appear to dominate the broadening as well as the coherence of the SC spectrum. SC generation uses PCF with all-normal dispersion for broad SC spectrum, flat top, and high coherence due to the main dominance of the self-phase modulation (SPM) effect followed by optical breaking (OWB). For the input pulses in the anomalous dispersion regime of PCF, the main dynamics of SCG include initial fission of the Nth-order soliton, self-steepening effect, intrapulse Raman scattering, and high-order dispersion [13]. Thus, controlling the dispersion property in the engineered PCFs is essential. SC generation is most effective when the obtained dispersion curve is flat and close to the zero-dispersion curve. At the same time, the effective mode area and attenuation are as small as possible [13].

In this work, we combined both ways including lattice modification and benzene infiltration into the hollow-core of PCF to optimize dispersion and other nonlinear properties. The circular lattice was chosen due to its high geometrical symmetry, which further enhances the light entering the core of the PCF. Benzene has a low attenuation over a wide spectral range from 0.5 to 14 μm although its nonlinear refractive index is similar to that of toluene or nitrobenzene (n_2= (0.6 to 5)×10^{-19} m^2/W). This results in a more stable spectrum and less attenuation over a wide wavelength range [14]. Our new structural design is to make the difference in air hole diameter and pitch in the innermost layer around the core from the other layers in the cladding. With such a structural design, we controlled the dispersion of the PCFs, obtaining both all-normal and anomalous dispersion regimes. More interestingly, we have achieved ultra-flat dispersion, as small as ± 0.484 ps/nm.km over a wide wavelength range. Furthermore, the small effective mode area resulting in high nonlinearity and very low attenuation make these PCFs quite an ideal nonlinear medium for SC applications.

2. Numerical Modeling of the PCFs

To design the structure of benzene-permeable hollow-core PCF and simulate their optical properties, we use Lumerical's Mode Solutions (LMS) software with vector full vector finite difference eigenmode (FDE) method. The advantage of this method is that the FDE process solves Maxwell's equations on a waveguide cross-sectional grid, the waveguide geometric mesh is divided into an infinite number of small rectangular parts. The boundary condition for the simulation is a perfectly matched layer, which allows strong absorption of outgoing waves from the computational region without any reflection.

The structural design of PCFs includes the following steps: First, the fused silica and benzene materials are entered into the data system by declaring the refractive index coefficients from equations (1) and (2). These are the Sellmeier [15] and Cauchy [16] equations representing the variation of the real parts of the refractive index of fused silica and benzene with wavelength. Next, we create a hollow-core circular lattice of PCF from the available data on the geometry of the structure and enter the calculated structural parameters into the data. Finally, benzene is filled into the hollow core of the PCF, and the air is chosen as the substrate for the parallel holes along the fiber.

Some of our previous publications [4, 8] have demonstrated the ability to control dispersion well by varying the air hole diameters of the layers, but the pitch remains unchanged. Thus, in this new design, the diameter d_1 of the air hole and the pitch Λ in the innermost layer near the core is different from the other layers in the cladding. The pitch of the innermost layer is set $\Lambda_1 = 1.095\Lambda$. The geometric cross-section of the PCF is shown in Fig. 1a. We simulate the optical properties of PCF according to the

variation of the filling factor d_1/Λ and pitch Λ in the wavelength range from 0.5 to 2.0 µm because of the wavelength limitation of fused silica. The d_1/Λ varies from 0.3 to 0.65 while Λ = 0.9, 1.0, 1.5, and 2.0 µm. Light is well confined within the core of the PCF, as depicted in Fig. 1b.

$$n^2_{\text{Benzene}}(\lambda) = 2.170184597 + 0.00059399\lambda^2 + \frac{0.02303464}{\lambda^2} + \frac{0.000499485}{\lambda^4} + \frac{0.000178796}{\lambda^6} \quad (1)$$

$$n^2_{\text{Fused silica}}(\lambda) = 1 + \frac{0.6694226\lambda^2}{\lambda^2 - 4.4801\times10^{-3}} + \frac{0.4345839\lambda^2}{\lambda^2 - 1.3285\times10^{-2}} + \frac{0.8716947\lambda^2}{\lambda^2 - 95.341482} \quad (2)$$

where λ is the excitation wavelength in micrometers, $n(\lambda)$ is the wavelength-dependent linear refractive index of materials.

The real parts of the refractive index of benzene and fused silica used in this paper versus wavelength are shown in Fig. 1c. In the investigated wavelength range, the real parts of the refractive index of benzene are always larger than fused silica. The larger the difference in refractive index between the coating and the core, the better the light confinement of the PCF.

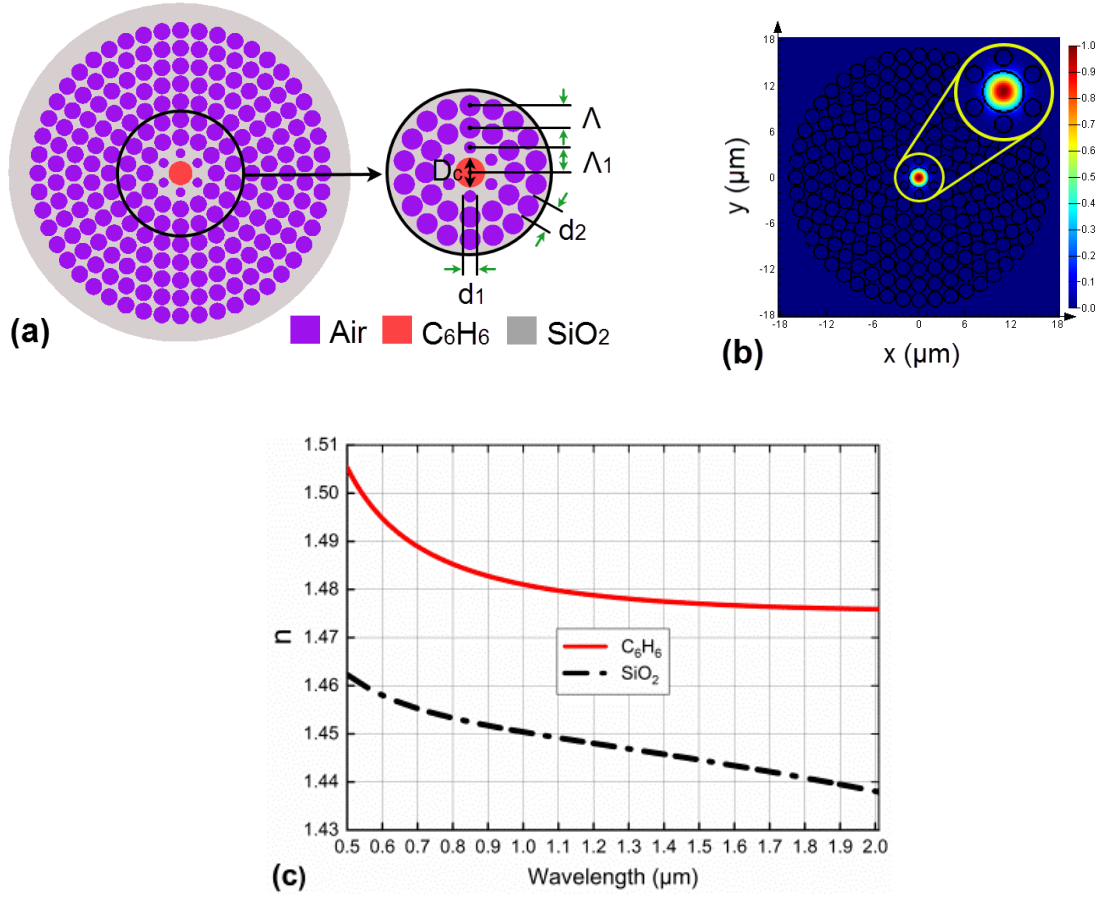

Figure 1. The geometrical structures of PCF with benzene-core (a), The light is well confined in the core of PCF (b), Real parts of the refractive index of benzene and fused silica (c).

3. Chromatic Dispersion and Nonlinear Properties of PCFs

The chromatic dispersion D(λ) of PCF can be easily computed from the derivative of the real part of the effective refractive index Re[n_{eff}] with respect to the wavelength λ and is determined by the following formula [17]:

$$D(\lambda) = -\frac{\lambda}{c}\frac{d^2\,\text{Re}\left[n_{\text{eff}}\right]}{d\lambda^2} \tag{3}$$

where c is the velocity of light in vacuum.

The optical pulse variation per unit distance of the propagation length is dominated by the dispersion property, so the design of PCFs with diverse dispersion will flexibly meet its application in SC. The variation of dispersion with wavelength is illustrated in Fig. 2.

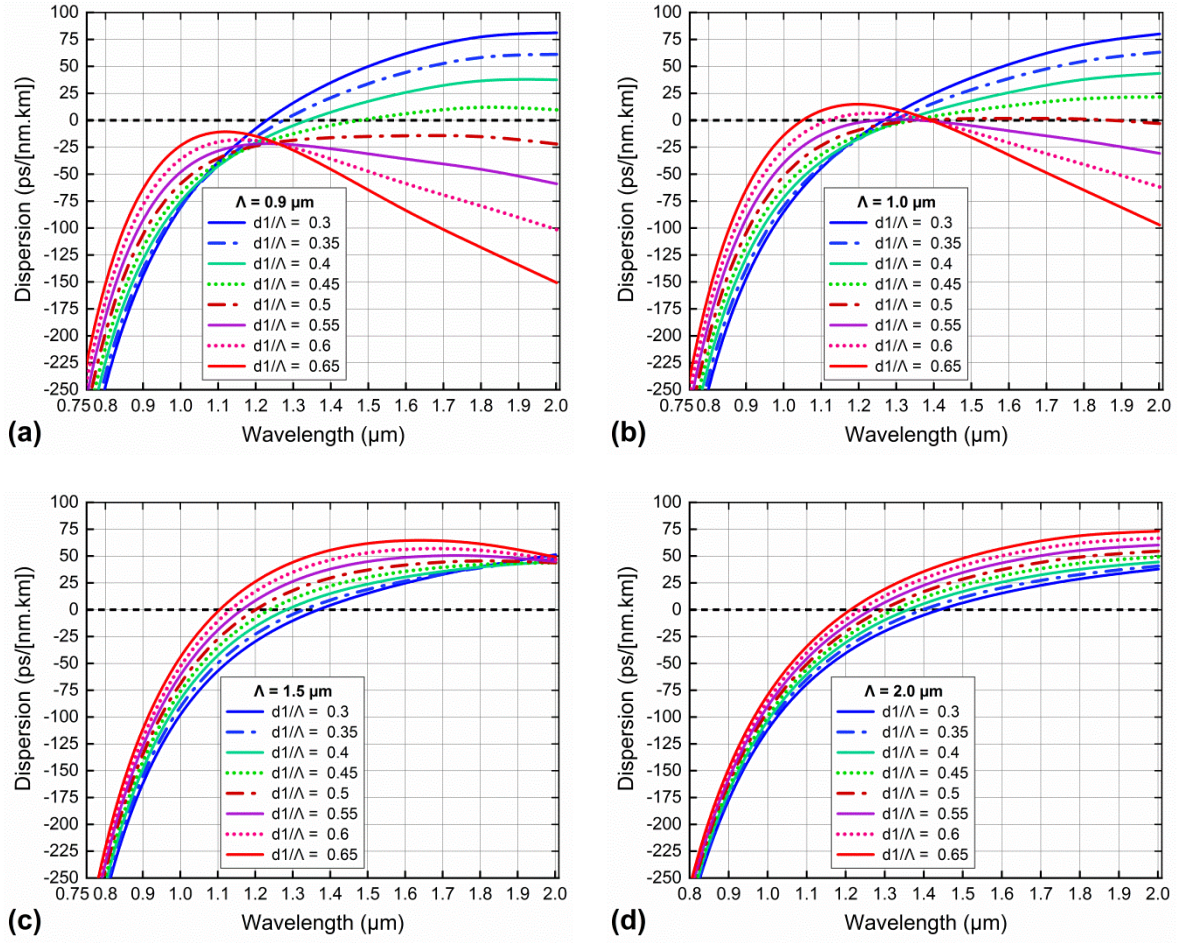

Figure 2. The dispersion characteristics of benzene-core PCFs with various d_1/Λ and Λ = 0.9 μm (a), Λ = 1.0 μm (b), Λ = 1.5 μm (c), and Λ = 2.0 μm (d).

The variation of chromatic dispersion is strongly influenced by the filling factor d_1/Λ and pitch Λ. Furthermore, the zero-dispersion wavelength (ZDW) also shifted to the low-frequency region, which is beneficial for choosing the wavelength of the excitation pulse in the SC. With the difference in structure

as described above, it is easy to achieve all-normal and anomalous dispersion profiles when Λ is small. For Λ = 0.9 μm, there are four anomalous dispersion curves corresponding to d_1/Λ less than 0.5. When d_1/Λ is larger, the dispersion curves lie completely below the zero-dispersion, i.e. the PCFs have an all-normal dispersion regime (Fig. 2a). Increasing Λ further, Λ = 1.0 μm, the all-normal dispersion curves gradually shift to the horizontal axis, they intersect the horizontal axis at two points, i.e. anomalous dispersion with two ZDWs occurs (Fig. 2b). Continuing to increase Λ (Λ = 1.5 and 2.0 μm), anomalous dispersions with two ZDWs no longer appear, instead anomalous dispersions with one ZDW completely dominate (Figs. 2c and d).

Interestingly, PCF with d_1/Λ = 0.5 and Λ = 0.9 μm (Fig. 2a) has an all-normal dispersion curve, ultra-flat, near-zero, and dispersion values as small as ±0.484 ps/nm.km over a fairly wide wavelength range of 450 nm (from 1.41 μm to 1.86 μm). The maximum point of this dispersion curve is very close to the wavelength of 1.55 μm, which is the common wavelength of lasers in practice. When Λ = 1.0 μm, this curve shifts upwards and intersects the zero-dispersion curve, becoming an ultra-flat anomalous dispersion curve with one ZDW, whose dispersion value is ±0.88 ps/nm.km in the wavelength region of 440 nm, spanning from 1.38 μm to 1.82 μm.

Although our previous publications [4, 8] have proven good dispersion control by varying the air hole diameters of layers in the cladding, we have not yet achieved near-zero, ultra-flat dispersion such as in this report. Compared with some other publications on ultra-flat dispersion of PCFs, our results are similar [18, 19] and even more optimal [20-22].

Table1. The values of ZDW of benzene-core PCFs with various values of d_1/Λ and Λ

PCF	Λ = 0.9 μm	Λ = 1.0 μm		Λ = 1.5 μm	Λ = 2.0 μm
d_1/Λ	ZDW_1	ZDW_1	ZDW_2	ZDW_1	ZDW_1
0.3	1.228	1.266		1.367	1.438
0.35	1.273	1.292		1.325	1.395
0.4	1.335	1.316		1.282	1.358
0.45	1.477	1.341		1.235	1.321
0.5		1.360	1.881	1.199	1.292
0.55		1.229	1.368	1.161	1.264
0.6		1.117	1.385	1.133	1.234
0.65		1.048	1.394	1.103	1.211

Normally, the pump wavelengths of the excitation pulses in SC generation are chosen close to the wavelength corresponding to the ZDW of the dispersion curve and satisfy the condition that the dispersion value is small. Therefore, the shift of the ZDW to the long-wavelength region, around 1.55 μm is of great significance in SC. The ZDW values of the PCFs are presented in Table 1. Some structures with flat dispersion and ZDW close to 1.55 μm wavelength are Λ = 0.9 μm, d_1/Λ = 0.45; Λ = 1.0 μm, d_1/Λ = 0.5; and Λ = 2.0 μm, d_1/Λ = 0.3.

The nonlinear coefficient is one of the parameters that govern the peak power of the input pulse in the SC generation, it also contributes to the emergence of new frequencies when the pulse interacts with the nonlinear medium such as PCF. So PCFs with higher nonlinearity give a broader SC spectrum with lower peak power. The nonlinear coefficient (γ) is calculated by the formula [23]:

$$\gamma(\lambda) = 2\pi \frac{n_2}{\lambda A_{\text{eff}}} \tag{4}$$

where A_{eff} is the effective mode area for the fundamental mode of the fiber and n_2 is the nonlinear refractive index of the fused silica. The effective mode area is a quantitative measure of the area that a waveguide or fiber mode effectively covers in the transverse dimensions and it can be computed by using the formula in [23] where E is the transverse electric field over the cross-section of the PCF.

$$A_{\text{eff}} = \frac{\left(\int_{-\infty}^{\infty}\int_{-\infty}^{\infty}|E|^2\,dxdy\right)^2}{\int_{-\infty}^{\infty}\int_{-\infty}^{\infty}|E|^4\,dxdy} \tag{5}$$

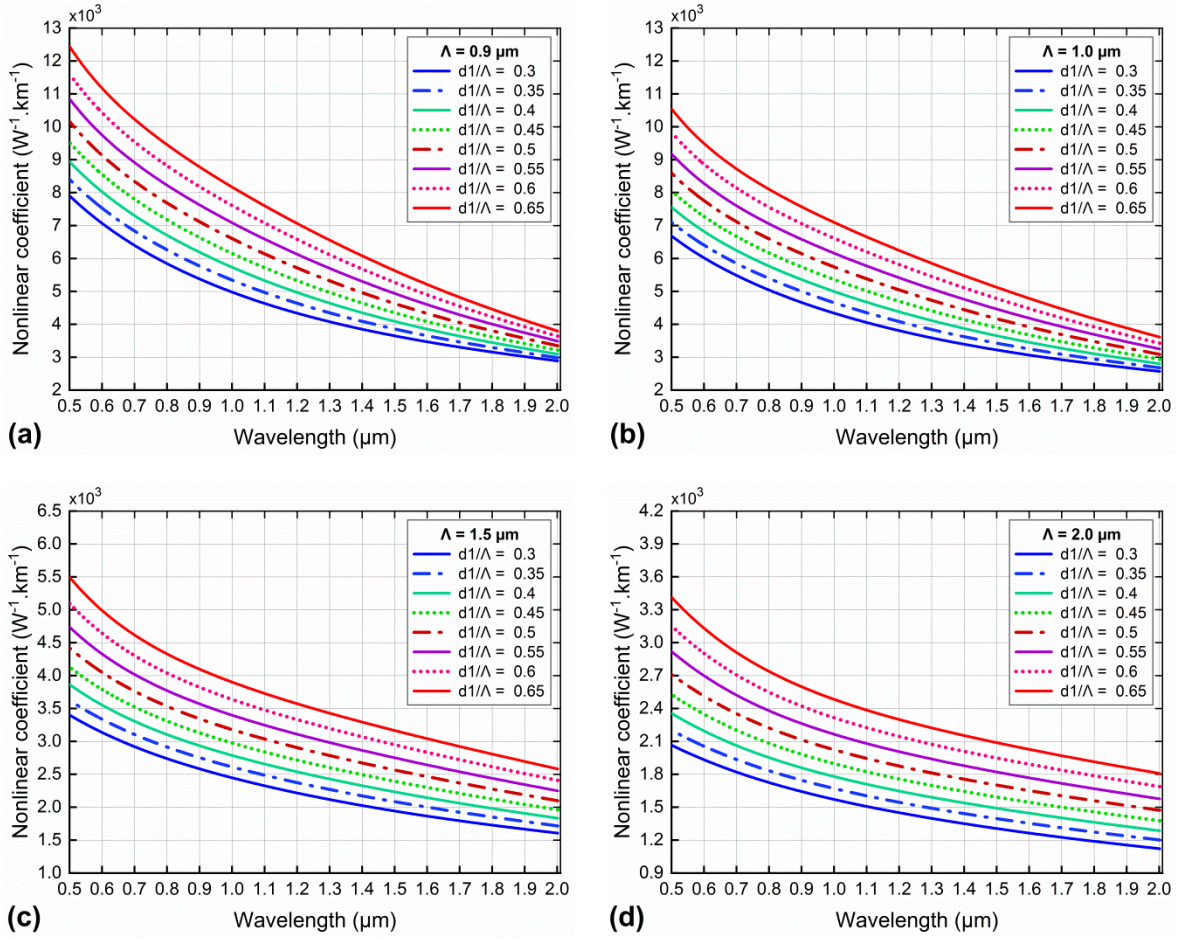

Figure 3. The nonlinear coefficient of benzene-core PCFs with various d_1/Λ and Λ = 0.9 μm (a), Λ = 1.0 μm (b), Λ = 1.5 μm (c), and Λ = 2.0 μm (d).

The nonlinear coefficients of PCFs infiltration with benzene are described in Fig. 3. In the short wavelength region, the value of the nonlinear coefficient is very high, up to several tens of thousands of $W^{-1}.km^{-1}$ and it gradually decreases as the wavelength increases. In the long-wavelength range, the nonlinear coefficient has a lower value because the modes are easily leaked to the cladding, but it still reaches several thousand $W^{-1}.km^{-1}$. Compared with some other publications [10-12, 24], we achieve a higher coefficient of nonlinearity.

For each fixed Λ, the nonlinear coefficient decreases with the increase of d_1/Λ. Similarly, when d_1/Λ is constant, an increase of Λ also reduces the nonlinear coefficient. The change in the core size of the PCFs ($D_c = 2\Lambda - 1.2d_1$) is the cause of this phenomenon, the larger the core PCFs the less light is confined in the core.

In equation (4), the effective mode area is inversely proportional to the nonlinear coefficient, so the variation of the effective mode area with respect to wavelength, in terms of d_1/Λ, and Λ is explained similarly. The effective mode area as a function of wavelength is displayed in Fig. 4.

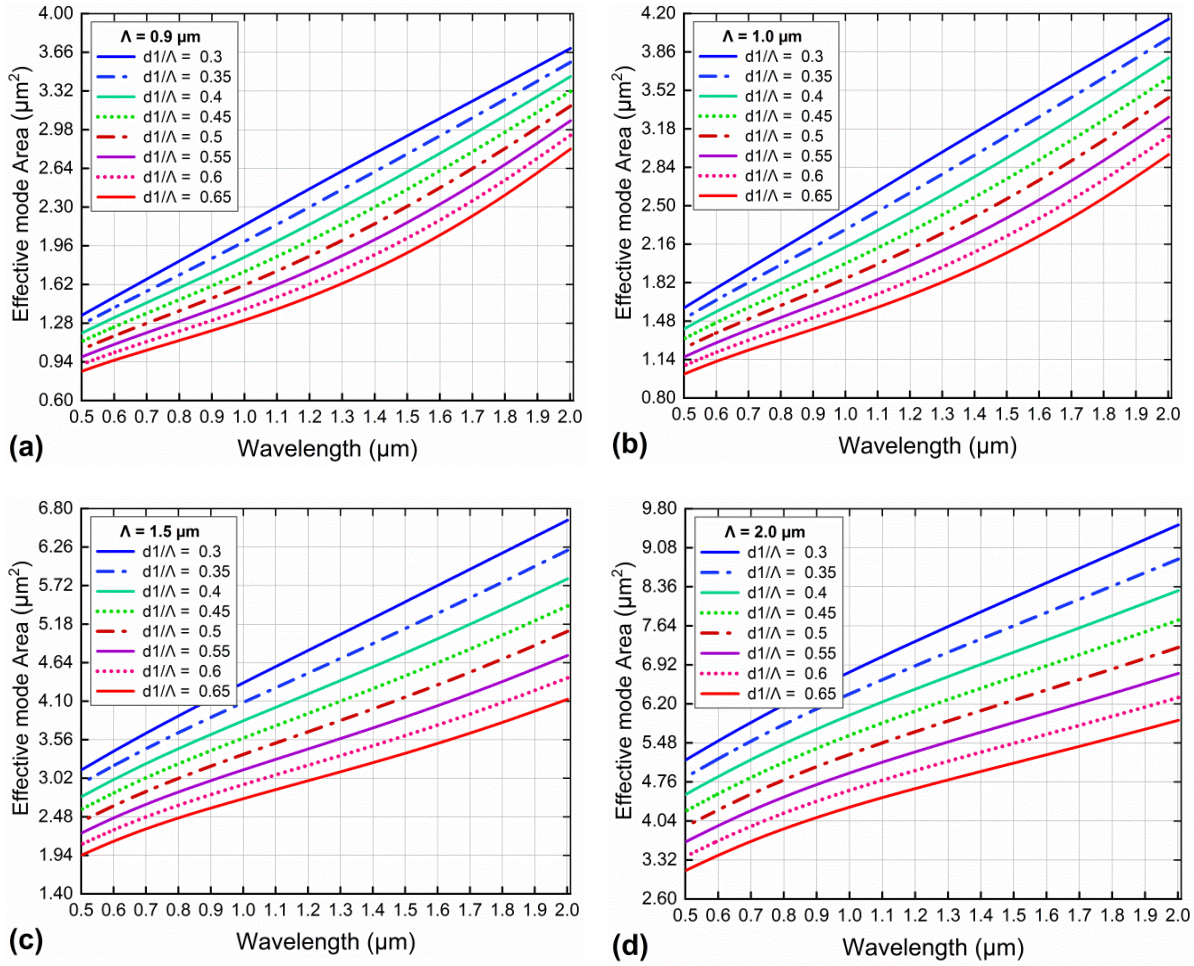

Figure 4. The effective mode area of benzene-core PCFs with various d_1/Λ and Λ = 0.9 μm (a), Λ = 1.0 μm (b), Λ = 1.5 μm (c), and Λ = 2.0 μm (d).

The values of the nonlinear coefficients and the effective mode area calculated at 1.55 μm wavelength are indicated in Table 2. The maximum and minimum values of the nonlinear coefficients are 5414.733 and 1285.42 $W^{-1}.km^{-1}$ corresponding to the minimum and maximum values of the effective mode area of 1,973 and 8,3 μm^2 for the structures Λ = 0.9 m, d_1/Λ = 0.65 and Λ = 2.0 m, d_1/Λ = 0.3.

Table 2. The nonlinear coefficient and the effective mode area at 1.55 μm wavelength

γ ($W^{-1}.km^{-1}$)				
$/\Lambda$	Λ = 0.9 μm	Λ = 1.0 μm	Λ = 1.5 μm	Λ = 2.0 μm
0.3	3553.793	3139.310	1903.482	1285.420
0.35	3749.795	3334.285	2042.493	1374.209
0.4	3967.206	3548.993	2189.202	1468.504
0.45	4209.587	3784.518	2347.336	1569.264
0.5	4473.610	4041.426	2515.422	1676.625
0.55	4761.887	4322.027	2697.047	1794.900
0.6	5077.015	4626.896	2891.507	1920.289
0.65	5414.733	4953.286	3103.959	2057.763
A_{eff} (μm^2)				
d_1/Λ	Λ = 0.9 μm	Λ = 1.0 μm	Λ = 1.5 μm	Λ = 2.0 μm
0.3	3.003	3.399	5.605	8.300
0.35	2.846	3.201	5.224	7.763
0.4	2.691	3.008	4.874	7.265
0.45	2.536	2.821	4.546	6.798
0.5	2.387	2.642	4.242	6.363
0.55	2.243	2.470	3.956	5.943
0.6	2.104	2.308	3.690	5.555
0.65	1.973	2.156	3.438	5.184

For the SC generations, the selection of PCFs with a reasonably small, flat dispersion is the essential factor, which is responsible for the output pulse characteristics. Furthermore, a PCF with high nonlinearity, small effective mode area, and low attenuation will fulfill the requirements to improve SC performance. However, it is difficult to optimize the PCF characteristics simultaneously, depending on the design to obtain PCFs with the expected optical properties. Based on the analysis of optical properties as above, we propose three fibers in favor of SC generation. The first fiber, #F_1 with Λ = 0.9 μm and d_1/Λ = 0.5, has all-normal dispersion, ultra-flat, near-zero, and it is expected to be able to generate SC with broad-spectrum, flat top, and coherence high. The pump wavelength was chosen as 1.55 μm which is very close to the maximum point of the dispersion curve. The second fiber, #F_2 with Λ = 1.0 μm and d_1/Λ = 0.5 has an ultra-flat anomalous dispersion, which can produce a broader SC spectrum than PCF with all-normal dispersion. The pump wavelength is 1.4 μm, which is larger than its ZDW. The third fiber, #F_3 with Λ = 2.0 μm and d_1/Λ = 0.5 has the flattest anomalous dispersion among the fibers with Λ = 2.0 μm. The pump wavelength was chosen as 1.45 μm because its ZDW is 1.438 μm. We choose two fibers with anomalous dispersion, #F_2 and #F_3 with the hope that their SC spectra are compared to consider how to create a broad SC spectrum of fiber with ultra-flat anomalous dispersion. The graphs of chromatic dispersion, nonlinearity coefficients, effective mode area, and attenuation of the proposed fibers are indicated in Fig. 5.

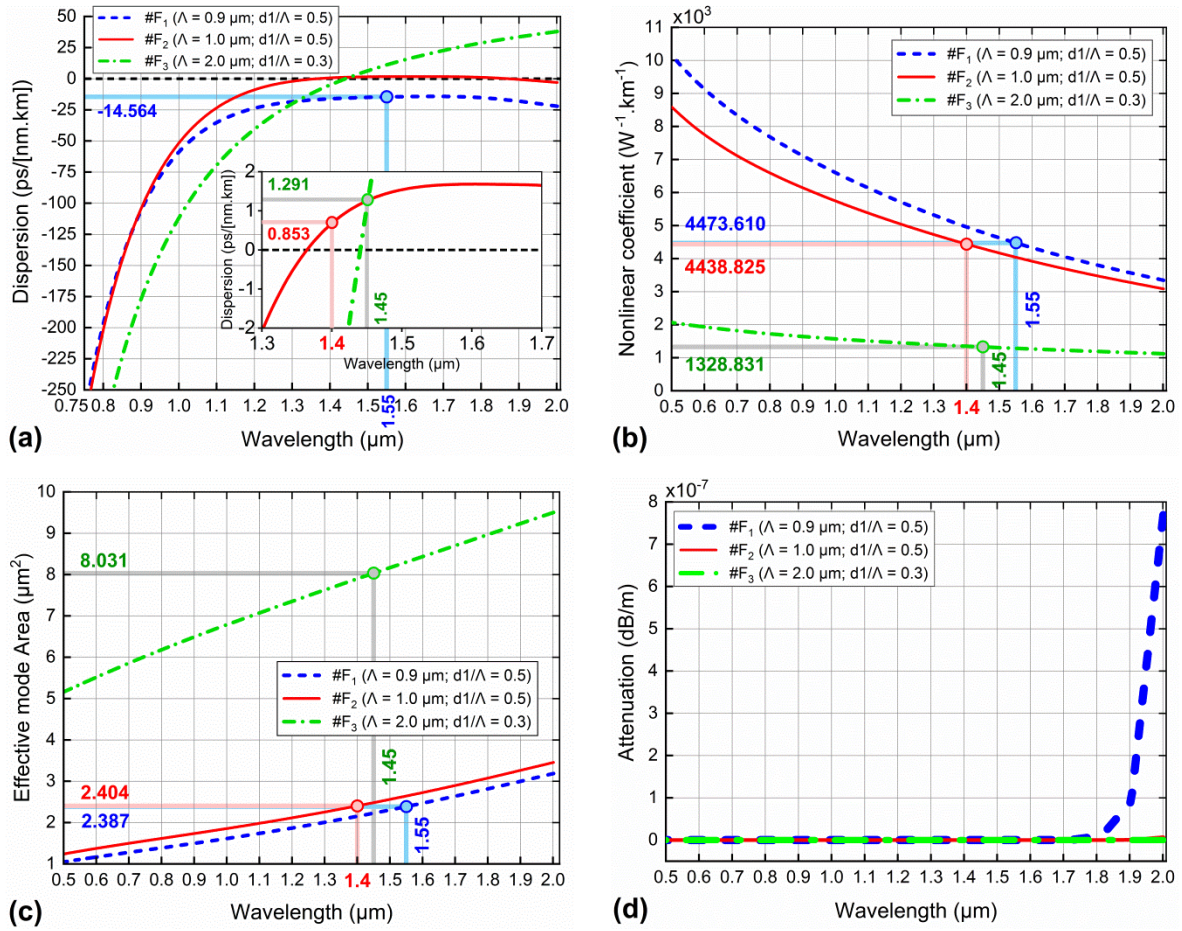

Figure 5. The chromatic dispersion (a), nonlinearity coefficient (b), effective mode area (c), and attenuation (d) of the proposed fibers.

The structural parameters of the proposed optimal fibers, as well as dispersion values, nonlinear coefficients, effective mode area, and attenuation at the pump wavelength, are manifested in Table 3. Among the three selected fibers, fiber #F_1 has the smallest core diameter, corresponding to the highest nonlinear coefficient 4473.61 $W^{-1}.km^{-1}$ and the smallest effective mode area of 2.387 μm^2. This fiber will enable a broad and flat SC spectrum with low peak power. #F_2 fiber has the smallest dispersion value of 0.853 ps/nm.km at the pump wavelength, which is predicted to produce the broadest SC spectrum in the ultra-flat, anomalous dispersion regime. Although #F_3 fiber has no ultra-flat dispersion profile, it has a relatively small dispersion value of 1.291 ps/nm.km at the pump wavelength in the anomalous dispersion regime. With the lowest attenuation of 2.602×10^{-21} dB/m, this fiber is also expected for a broad SC spectrum. Compared with the work [24] about PCF filled with benzene, the fibers proposed in this paper have more optimal dispersion properties, near-zero super-flat dispersion for both all-normal and anomalous dispersion are obtained. This also demonstrates the outstanding results of the proposed fibers compared with the works [8–12] which have proven dispersion control with suitable modification lattice parameters but the near zero utral-flat dispersion has not yet been achieved. It can be seen that each of the #F_1 to #F_3 fibers has distinct properties and SC applications. They are good candidates for SC generation applications with broad spectrum and low peak power.

Table 3. The structure parameters and the characteristic quantities of proposed PCFs at the pump wavelength

#	Λ (μm)	d_1/Λ	D_c (μm)	Pump Wavelength (μm)	D (ps/nm.km)	γ ($W^{-1}.km^{-1}$)	A_{eff} (μm^2)	L_k (dB/m)
$\#F_1$	0.9	0.5	1.26	1.55	–14.564	4473.610	2.387	7.320×10^{-12}
$\#F_2$	1.0	0.5	1.40	1.40	0.853	4438.825	2.404	4.535×10^{-17}
$\#F_3$	2.0	0.3	3.28	1.45	1.291	1328.381	8.031	2.602×10^{-21}

4. Conclusion

With a new design, the distance from the core to the first layer of air holes near the core was modified compared to others, we have achieved two ultra-flat all-normal and anomalous dispersions regimes in a wide wavelength range. Dispersion differences as small as ± 0.484 ps/nm.km in 450 nm wavelength range and ± 0.88 ps/nm.km in the 440 nm wavelength region are the outstanding advantages of these benzene-infiltrated circular lattice PCFs. In particular, very small attenuation of about 10^{-21} dB/m is found in the optimized structures. The proposed three fibers with high nonlinear coefficient and small effective mode area are favorable conditions for the application of PCFs in SC generation. Our new numerical simulation results will contribute to the direction of SC applications in theory as well as in experiments, suitable for low-cost all-fiber laser systems.

Acknowledgments

This research is funded by the University of Education, Hue University, under grant number T.23 – TN – 01.

References

[1] R. R. Alfano, S. L. Shapiro, Emission in the Region 4000–7000 Å Via Four-Photon Coupling in Glass, Physical Review Letters, Vol. 24, No. 11, 1970, pp. 584-587, https://doi.org/10.1103/PhysRevLett.24.584.

[2] J. M. Dudley, G. Genty, S. Coen, Supercontinuum Generation in Photonic Crystal Fiber, Review of Modern Physics, Vol. 78, 2006, pp. 1135-1184, https://doi.org/10.1103/RevModPhys.78.1135.

[3] F. Begum, Y. Namihira, T. Kinjo, S. Kaijage, Supercontinuum Generation in Square Photonic Crystal Fiber with Nearly Zero Ultra-Flattened Chromatic Dispersion and Fabrication Tolerance Analysis, Optics Communications, Vol. 284, No. 4, 2011, pp. 965-970, https://doi.org/10.1016/j.optcom.2010.10.029.

[4] N. T. Thuy, H. T. Duc, L. T. Bao Tran, D. V. Trong, C. V.Lanh, Optimization of Optical Properties of Toluene-Core Photonic Crystal Fibers with Circle Lattice for Supercontinuum Generation, Journal of Optics, 2022, https://doi.org/10.1007/s12596-021-00802-y.

[5] A. A. Nair, C. S. Boopathi, M. Jayaraju, M. S. M. Rajan, Numerical Investigation and Analysis of Flattened Dispersion for Supercontinuum Generation at Very Low Power Using Hexagonal Shaped Photonic Crystal Fiber (H-PCF), Optik, Vol. 179, 2019, pp. 718-725, https://doi.org/10.1016/j.ijleo.2018.11.021.

[6] M. A. Sadath, M. S. Islam, M. S. Hossain, M. Faisal, Ultra-high Birefringent Low Loss Suspended Elliptical Core Photonic Crystal Fiber for Terahertz Applications, Applied Optics, Vol. 59, No. 30, 2020, pp. 9385-9392, https://doi.org/10.1364/AO.402530.

[7] A. Sharafali, K. Nithyanandan, A Theoretical Study on the Supercontinuum Generation in a Novel Suspended Liquid Core Photonic Crystal Fiber, Applied Physics B, Vol. 126, 2020, pp. 55-66, https://doi.org/10.1007/s00340-020-7403-9.

[8] C. V. Lanh, N. T. Thuy, H. T. Duc, L. T. Bao Tran, V. T. M. Ngoc, D. V. Trong, L. C. Trung, H. D. Quang, D. Q. Khoa, Comparison of Supercontinuum Spectrum Generating by Hollow Core PCFs Filled with Nitrobenzene

with Different Lattice Types, Optical and Quantum Electronics, Vol. 54, No. 5, 2022, pp. 300-316, https://doi.org/10.1007/s11082-022-03667-y.

[9] L. T. B. Tran, N. T. Thuy, V. T. M. Ngoc, L. C. Trung, L. V. Minh, C. L. Van, D. X. Khoa, C. V. Lanh, Analysis of Dispersion Characteristics of Solid-Core PCFs with Different Types of Lattice in the Claddings, Infiltrated with Ethanol, Photonics Letters of Poland, Vol. 12, No. 4, 2020, pp. 106-108, https://doi.org/10.4302/plp.v12i4.1054.

[10] C. V. Lanh, H. V. Thuy, C. L. Van, K. Borzycki, D. X. Khoa, T. Q. Vu, M. Trippenbach, R. Buczyński, J. Pniewski, Supercontinuum Generation in Photonic Crystal Fibers Infiltrated with Nitrobenzene, Laser Physics, Vol. 30, No. 3, 2020, pp. 035105-035113, https://doi.org/10.1088/1555-6611/ab6f09.

[11] C. V. Lanh, H. V. Thuy, C. L. Van, K. Borzycki, D. X. Khoa, T. Q. Vu, M. Trippenbach, R. Buczyński, J. Pniewski, Optimization of Optical Properties of Photonic Crystal Fibers Infiltrated with Chloroform for Supercontinuum Generation, Laser Physics, Vol. 29, No. 7, 2019, pp. 075107, https://doi.org/10.1088/1555-6611/ab2115.

[12] C. V. Lanh, A. Anuszkiewicz, A. Ramaniuk, R. Kasztelanic, D. X. Khoa, M. Trippenbach, R. R. Buczynski, Supercontinuum Generation in Photonic Crystal Fibres with Core Filled with Toluene, Journal of Optics, Vol. 19, No. 12, 2017, pp. 125604, https://doi.org/10.1088/2040-8986/aa96bc.

[13] J. M. Dudley, J. R. Taylor, Supercontinuum Generation in Optical Fibers, Cambridge University Press, Cambridge, 2010, https://doi.org/10.1017/CBO9780511750465.

[14] D. Churin, T. N. Nguyen, K. Kieu, R. A. Norwood, N. Peyghambarian, Mid-Ir Supercontinuum Generation in an Integrated Liquid-Core Optical Fiber Filled with CS_2, Optical Materials Express, Vol. 3, No. 9, 2013, pp. 1358-1364, https://doi.org/10.1364/OME.3.001358.

[15] C. Z. Tan, Determination of Refractive Index of Silica Glass for Infrared Wavelengths by Ir Spectroscopy, Journal of Non-Crystalline Solids, Vol. 223, No. 1-2, 1998, pp. 158-163, https://doi.org/10.1016/s0022-3093(97)00438-9.

[16] K. Moutzouris, M. Papamichael, S. C. Betsis, I. Stavrakas, G. Hloupis, D. Triantis, Refractive, Dispersive and Thermo-Optic Properties of Twelve Organic Solvents in the Visible and Near-Infrared, Applied Physics B, Vol. 116, No. 3, 2014, pp. 617-622, https://doi.org/10.1007/s00340-013-5744-3.

[17] Y. S. Lee, C. G. Lee, F. Bahloul, S. Kim, K. Oh, Simultaneously Achieving a Large Negative Dispersion and a High Birefringence Over Er and Tm Dual Gain Bands in a Square Lattice Photonic Crystal Fiber, Journal of Lightwave Technology, Vol. 37, No. 4, 2019, pp. 1254-1263, https://doi.org/10.1109/JLT.2019.2891756.

[18] A. Medjouri, E. B. Meraghni, H. Hathroubi, D. Abed, L. M. Simohamed, O. Ziane, Design of Zblan Photonic Crystal Fiber with Nearly Zero Ultra-Flattened Chromatic Dispersion for Supercontinuum Generation, Optik, Vol. 135, 2017, pp. 417-425, https://doi.org/10.1016/j.ijleo.2017.01.082.

[19] A. Medjouri, L. M. Simohamed, O. Ziane, A. Boudrioua, Z. Becer, Design of a Circular Photonic Crystal Fiber with Flattened Chromatic Dispersion Using a Defected Core and Selectively Reduced Air Holes: Application to Supercontinuum Generation at 1.55 μm, Photonics and Nanostructures - Fundamentals and Applications, Vol. 16 2015, pp. 43-50, https://doi.org/10.1016/j.photonics.2015.08.004.

[20] H. V. Le, V. L. Cao, H. T. Nguyen, A. M. Nguyen, R. Buczyński, R. Kasztelanic, Application of Ethanol Infiltration for Ultra-Flattened Normal Dispersion in Fused Silica Photonic Crystal Fibers, Laser Physics, Vol. 28, No. 11, 2018, pp. 115106, https://doi.org/10.1088/1555-6611/aad93a.

[21] T. Huang, Q. Wei, Z. Wu, X. Wu, P. Huang, Z. Cheng, P. P. Shum, Ultra-Flattened Normal Dispersion Fiber for Supercontinuum and Dissipative Soliton Resonance Generation at 2 μm, IEEE Photonics Journal, Vol. 11, No. 3, 2019, pp. 7101511, https://doi.org/10.1109/JPHOT.2019.2915265.

[22] P. Kumar, K. F. Fiaboe, J. S. Roy, Design of Nonlinear Photonic Crystal Fibers with Ultra-Flattened Zero Dispersion for Supercontinuum Generation, ETRI Journal, Vol. 42, No. 2, 2020, pp. 282-291, https://doi.org/10.4218/etrij.2019-0024.

[23] G. Agrawal, Nonlinear Fiber Optics (Fifth Edition), Elsevier, Amsterdam, 2013, https://doi.org/10.1016/C2011-0-00045-5.

[24] C. V. Lanh, H. V. Thuy, C. L. Van, K. Borzycki, D. X. Khoa, T. Q. Vu, M. Trippenbach, R. Buczyński, J. Pniewski, Supercontinuum Generation in Benzene-Filled Hollow-Core Fibers, Optical Engineering, Vol. 60, No. 11, 2021, pp. 116109, https://doi.org/10.1117/1.OE.60.11.116109.